

Effective conductivity of partially sintered solids

J. R. Dryden

Department of Mechanical and Materials Engineering, The University of Western Ontario, London, Ontario N6A 5B9, Canada

F. W. Zok^{a)}

Department of Materials, The University of California, Santa Barbara, California 93106

(Received 28 May 2003; accepted 7 October 2003)

An analytical model to predict the effective conductivity of a partially sintered solid is presented. It is based on an analysis of heat flow through a spherical particle embedded in a self-consistent matrix. Determination of the effective conductivity reduces to solving an integral equation, and a numerical solution of this equation is presented. In the limiting cases wherein the contact size is either small or comparable to the particle size, approximate analytical results are obtained which agree very well with the numerical solution. Furthermore, when pieced together, the two solutions are found to describe the effective conductivity over the entire range of contact sizes. © 2004 American Institute of Physics. [DOI: 10.1063/1.1630360]

I. INTRODUCTION

There has been a considerable amount of research directed toward predicting the effective thermal conductivity of porous and granular solids.^{1–10} In most of these treatments,^{3–7} it has been assumed that contacts between particles are sufficiently small so that the constriction resistance to heat flow corresponds to a contact spot separating two infinite half spaces.¹¹ This treatment is reasonable in the analysis of granular solids where the contact areas depend upon Hertzian mechanics. However, in the case of partially sintered solids, the finite contact size must be taken into account. Although there have been two numerical studies,^{9,10} this problem has received less attention.

Here, a calculation of the self-consistent type, where the heat flow through a sphere embedded in a self-consistent matrix, is presented. No other shape for equiaxed particles seems to offer any chance of an analytical solution. Similar to the calculation done by Argento and Bouvard,⁹ we take two contacts per sphere. These two caps are held at a self-consistent temperature, and the remaining portion of the sphere surface is adiabatic.

II. PRELIMINARY COMMENTS

From a macroscopic viewpoint, the porous solid is isotropic with respect to heat flow and its effective conductivity is k_e . Consequently, only heat flow in one direction needs to be analyzed. Here, heat flow in the Z direction is considered, and the apparent temperature is written as $T_e = CZ$. On a finer scale, the microstructure is nonuniform, and flow pattern is tessellated. In the simplest case, there are two phases: Solid particles with thermal conductivity k , and a gas phase with thermal conductivity k_g . A typical particle has a portion of its surface surrounded by gas with the remainder of its surface being in contact with its nearest neighbors. Let ρ be equal to the ratio of the contact radius to solid particle radius.

For sufficiently small values of ρ , the flow constriction through the solid contacts becomes severe and the heat flow is predominantly through the gas phase. On the other hand, it has been shown by Batchelor,⁴ that when $k\rho \gg k_g$, the heat flow through the gas phase is negligible. This condition is satisfied in most partially sintered solids.

Initially, the individual solid particles are approximately spherical. However, as sintering proceeds, the shape of each particle becomes irregular. If the particles remain equiaxed, it is useful to consider a “test” region that contains an average representative particle. The analysis presented here is concerned with analyzing the temperature field in this representative test region, and then relating this field to obtain an estimate for the effective conductivity. In a calculation of this type, neither the particle radius a nor the magnitude C of the thermal gradient, affects the estimate for k_e . Consequently, it is convenient to define dimensionless variables $z \equiv Z/a$, and $T_e \equiv T_e/Ca$. Using these definitions,

$$T_e \equiv \frac{T_e}{Ca} = z. \quad (1)$$

From this point onward in the article, all spatial variables and temperatures are dimensionless.

III. TEMPERATURE WITHIN THE TEST PARTICLE

To make the problem tractable, the shape of the test particle is taken as being a sphere having a radius equal to a . In view of the spatial scaling, the sphere has a dimensionless unit radius, and the dimensionless temperature in the particle is designated by T . For simplicity, the origin is placed at the center of the particle. Spherical coordinates (r, θ) are used where r is the distance from the center of the sphere and θ is the angle measured from the z axis. The temperature T must satisfy Laplace's equation

$$\nabla^2 T = 0. \quad (2)$$

^{a)}Electronic mail: zok@engineering.ucsb.edu

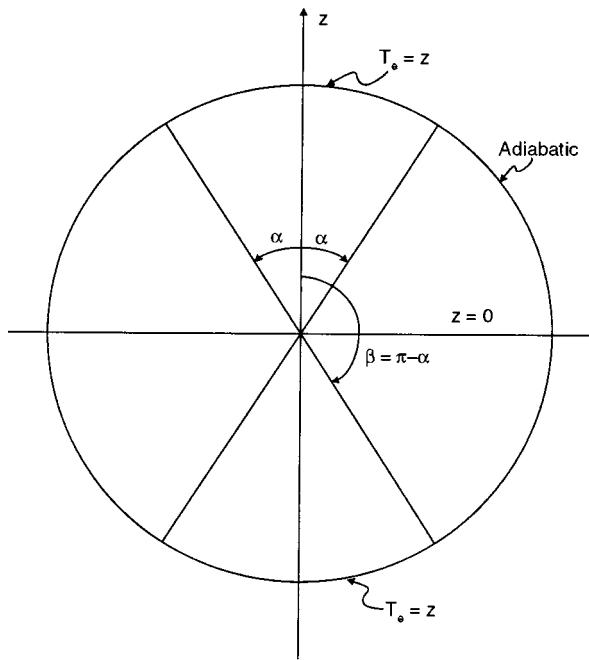


FIG. 1. Spherical test particle where the polar caps are symmetrical, i.e., $\beta = \pi - \alpha$ so that the temperature is an odd function of z .

The test particle is shown in Fig. 1, and on the surface, $r = 1$, the following boundary conditions are imposed. Within the equatorial region, i.e., $\alpha < \theta < \beta$, there is no radial flow and the boundary condition is then

$$\frac{\partial T}{\partial r} = 0 \quad (\beta > \theta > \alpha). \tag{3}$$

The apparent overall temperature $T_e = z$, and the surface of the sphere corresponds to $z = \cos \theta$. Therefore, on the north and south polar caps subtending the cone of angle 2α , the boundary condition

$$T = \cos \theta \quad (\alpha > \theta \geq 0, \pi \geq \theta > \beta), \tag{4}$$

is imposed. The temperature in the test sphere is written in the form

$$T = rP_1(\cos \theta) - \sum_{n=1}^{\infty} \frac{1+2n}{n} C_n P_n(\cos \theta) r^n, \tag{5}$$

where the terms $P_n(\cos \theta)$ are Legendre's polynomials. The temperature is an odd function of z so that only the terms, $n = 1, 3, 5, \dots$ are taken. The expression for T satisfies Laplace's equation, and the coefficients C_n are found using the two boundary conditions that are prescribed above. Using these two boundary conditions, it is found that the coefficients C_n must satisfy the following conditions:

$$\sum_{n=1}^{\infty} C_n (1 + H_n) P_n(\cos \theta) = 0 \quad (\alpha > \theta \geq 0, \pi \geq \theta > \beta) \tag{6}$$

$$\sum_{n=1}^{\infty} C_n (1 + 2n) P_n(\cos \theta) = 6\lambda P_1(\cos \theta) \quad (\beta > \theta > \alpha), \tag{7}$$

where the various coefficients are defined by

$$H_n = \frac{1}{2n}, \tag{8}$$

$$\lambda = \frac{1}{6}. \tag{9}$$

The relations in Eqs. (6) and (7) are referred to as triple series relations.^{12,13} The adjective "triple" arises from the fact that there are three different zones: (i) $\alpha > \theta \geq 0$, (ii) $\beta > \theta > \alpha$, and (iii) $\pi \geq \theta > \beta$. These mixed boundary value problems are generally more difficult than the standard problems where there is only a single condition over the entire surface. The aim is to find the coefficients C_n that satisfy the triple relations.

Owing to the symmetry of the present problem, the temperature is antisymmetric with respect to the plane $z = 0$ so that the Legendre coefficients $C_0, C_2, C_4, \dots, C_{2n}$ must vanish. As described by Collins,¹² in order to determine the Legendre coefficients, it is necessary to write $C_n = A_n + B_n$ and it follows that

$$C_n = A_n + B_n \quad \text{and} \quad B_n = -(-1)^n A_n. \tag{10}$$

The triple relations in Eqs. (6) and (7) are written as

$$\sum_{n=0}^{\infty} (A_n + B_n)(1 + H_n) P_n(\cos \theta) = 0 \quad (\alpha > \theta \geq 0), \tag{11}$$

$$\sum_{n=0}^{\infty} A_n (1 + 2n) P_n(\cos \theta) - 3\lambda P_1(\cos \theta) = 0 \quad (\pi \geq \theta > \alpha), \tag{12}$$

$$\sum_{n=0}^{\infty} B_n (1 + 2n) P_n(\cos \theta) - 3\lambda P_1(\cos \theta) = 0 \quad (\beta > \theta \geq 0), \tag{13}$$

$$\sum_{n=0}^{\infty} (A_n + B_n)(1 + H_n) P_n(\cos \theta) = 0 \quad (\pi \geq \theta > \beta). \tag{14}$$

The coefficients A_0, B_0 are not equal to zero so that the lower limit on the summation has been changed. To avoid objection over the possibility of division by zero, the term $H_0 \equiv 1$; this definition is inconsequential because $A_0 + B_0 = 0$. Owing to the symmetry of the problem, only the first two equations [Eqs. (11) and (12)] need to be considered.

It is known that the Legendre polynomials can be represented by the Mehler-Dirichlet integrals

$$P_n(\cos \theta) = \frac{\sqrt{2}}{\pi} \int_{t=0}^{\theta} \frac{\cos[(n+1/2)t] dt}{\sqrt{\cos t - \cos \theta}}, \tag{15}$$

$$= \frac{\sqrt{2}}{\pi} \int_{t=0}^{\pi} \frac{\sin[(n+1/2)t] dt}{\sqrt{\cos \theta - \cos t}}. \tag{16}$$

The representation for $P_n(\cos \theta)$ in Eq. (15) is used in Eq. (11) and, after interchanging the order of integration and summation, it follows that

$$\int_{t=0}^{\theta} \frac{dt}{\sqrt{\cos t - \cos \theta}} \left\{ \sum_{n=0}^{\infty} (A_n + B_n)(1 + H_n) \times \cos(n + 1/2)t \right\} = 0. \tag{17}$$

Similarly, the representation for $P_n(\cos \theta)$ in Eq. (16) is used in Eq. (12) and, after interchanging the order of integration and summation, it follows that

$$\int_{t=0}^{\pi} \frac{dt}{\sqrt{\cos \theta - \cos t}} \times \left\{ \frac{d}{dt} \left[\sum_{n=0}^{\infty} A_n \cos(n + 1/2)t - \lambda \cos 3t/2 \right] \right\} = 0. \tag{18}$$

Equations (17) and (18) can be solved using Eqs. (2.3.5) and (2.3.6) in Ref. 13. In both cases, the quantities within the $\{\dots\}$ must vanish. In Eq. (18), the portion within $[\dots] = D$ and the constant $D = 0$; this follows by noting that the expression within $[\dots]$ vanishes at $t = \pi$. Thus, the two results

$$\sum_{n=0}^{\infty} (A_n + B_n)(1 + H_n) \cos[(n + 1/2)t] = 0 \quad (\alpha > t \geq 0), \tag{19}$$

$$\sum_{n=0}^{\infty} A_n \cos[(n + 1/2)t] - \lambda \cos(3t/2) = 0 \quad (\pi \geq t > \alpha), \tag{20}$$

are obtained. Here, the coefficient A_n is found and once this is known the other two coefficients, C_n, B_n can be found by use of Eq. (10). To find A_n , an unknown function $j(t)$ is defined as follows

$$\sum_{n=0}^{\infty} A_n \cos\left[\left(n + \frac{1}{2}\right)t\right] = \begin{cases} \lambda \cos(3t/2) - j(t)/2 & (\alpha > t \geq 0) \\ \lambda \cos(3t/2) & (\pi \geq t > \alpha) \end{cases}. \tag{21}$$

The functions $\cos(n + 1/2)t$ are orthogonal over the interval $(0 \leq t \leq \pi)$ and thus the coefficient A_n is

$$A_n = \lambda \delta_{1n} - \frac{1}{\pi} \int_{u=0}^{\alpha} j(u) \cos\left[\left(n + \frac{1}{2}\right)u\right] du, \tag{22}$$

where $\delta_{1n} = 0$ when $n \neq 1$. Expressions (21) and (10) are then substituted into Eq. (19) to obtain

$$j(t) + 2 \sum_{n=0}^{\infty} A_n \{(-1)^n - H_n[1 - (-1)^n]\} \cos\left[\left(n + \frac{1}{2}\right)t\right] = 2\lambda \cos\left(\frac{3t}{2}\right). \tag{23}$$

Using the expression for A_n , and interchanging the order of summation and integration, Eq. (24) is found for the determination of $j(t)$:

$$j(t) = \cos(3t/2) + \frac{1}{\pi} \int_0^{\alpha} j(u) J(u, t) du \quad \text{where } (\alpha > t \geq 0). \tag{24}$$

The kernel $J(u, t) = K(t - u) + K(t + u)$ and $K(\xi)$ is

$$K(\xi) = \sum_{n=0}^{\infty} \{(-1)^n - H_n[1 - (-1)^n]\} \cos\left[\left(n + \frac{1}{2}\right)\xi\right] = \frac{1}{4} \left\{ 2 \sec\left(\frac{\xi}{2}\right) + \pi \sin\left|\frac{\xi}{2}\right| + \cos\left(\frac{\xi}{2}\right) \ln \left[\tan^2\left(\frac{\xi}{2}\right) \right] \right\}. \tag{25}$$

The closed forms for the infinite summations in Eq. (25) can be found from the results given in standard tables.¹⁴ For general values of α , the function $j(t)$ can only be found by a numerical treatment.

To summarize this section, the function $j(t)$ is a solution of the integral Eq. (24). The coefficients A_n are then found from Eq. (22) and the odd Legendre–Fourier series coefficients $C_{2n+1} = 2A_{2n+1}$. Finally, these coefficients are used in Eq. (5) to find the temperature.

IV. POWER EQUIVALENT CONDUCTIVITY

On the macroscopic level, the dimensionless apparent temperature, $T_e = z$, is given in Eq. (1). The thermal “power” P (which here has the same units as the conductivity), expended within the test volume V is expressed by the integral

$$P = k_e \int_V \text{grad } T_e \cdot \text{grad } T_e dV = k_e V.$$

The test volume V is comprised of two phases and, if there is negligible flow through the gas phase, then P is due to the power expended in the solid sphere. The power P can be alternatively written as

$$P = k \int_{V_s} \text{grad } T \cdot \text{grad } T dV,$$

where $V_s = 4\pi/3$ is the dimensionless volume of the sphere. Upon equating these two expressions for P , the power equivalent thermal conductivity is

$$k_e = kf\sigma, \tag{26}$$

where $f = V_s/V$ is the volume fraction of solid, and the conductance σ is defined as

$$\sigma = \frac{1}{V_s} \int_{V_s} \text{grad } T \cdot \text{grad } T dV. \tag{27}$$

The conductance σ is equal to the average squared magnitude of the temperature gradient within the sphere. In this expression, the volume integral can be converted to an integral over the surface of the sphere by the use of the divergence theorem. In view of the boundary conditions in Eqs. (3) and (4), along with the orthogonal nature of the Legendre polynomials, it follows after substituting the series in Eq. (5) into the surface integral that $\sigma = 1 - 3C_1$. The coefficient $C_1 = 2A_1$ and using the expression for A_1 in Eq. (22), the expression for σ is found as

$$\sigma = \frac{6}{\pi} \int_{u=0}^{\alpha} j(u) \cos\left(\frac{3u}{2}\right) du. \tag{28}$$

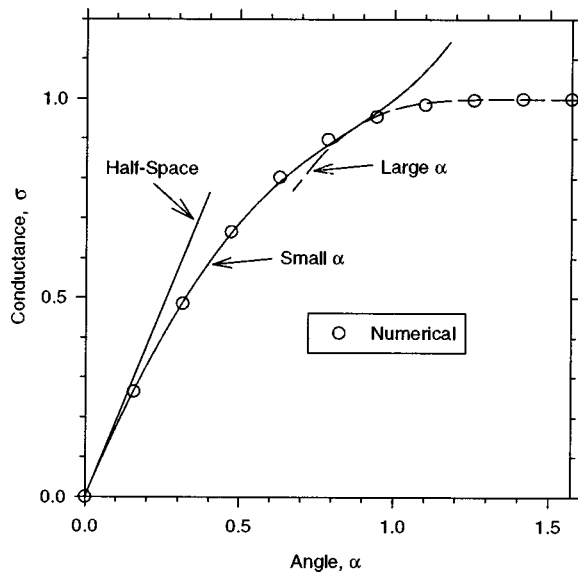


FIG. 2. The conductance σ as a function of the cap angle α . The symbols \circ are obtained by numerical integration. [The solid line labeled “small α ” is obtained from Eq. (30). The results of Eq. (31) represent the half-space approximation. Finally, the dashed line labeled “large α ”, represents the prediction of Eq. (36)].

To evaluate this conductance, the function $j(t)$ is found by numerically solving the integral Eq. (24) for the following ten values of α : $\pi/20, 2\pi/20, 3\pi/20, \dots, \pi/2$. For each value of α , the region $0 < u < \alpha$ is subdivided into 60 segments (this is found to give sufficiently accurate results), and a set of 60 linear equations is generated using Eq. (24). This set of 60 equations is then solved to find $j(t)$ at the discrete increments, $t = t_1, t_2, \dots, t_{60}$, within the interval $0 < t < \alpha$. The values, $j(t_1), j(t_2), \dots, j(t_{60})$, are then used to evaluate σ and the results are shown by the symbols in Fig. 2.

A. Approximate solution for σ when $\alpha < 1$

If α is small, the integral equation is amenable to an iterative solution. Using the expression for $j(t)$ given in Eq. (24), the conductance can be rewritten as

$$\sigma = \frac{3}{\pi} \left\{ \alpha + \frac{\sin 3\alpha}{3} \right\} + \frac{6}{\pi^2} \int_0^\alpha \int_0^\alpha J(u,t)j(u) \cos\left(\frac{3t}{2}\right) dudt. \tag{29}$$

When α becomes sufficiently small, the function $j(u) \approx \cos(3u/2)$, and the kernel can be approximated by its singular portion $J(u,t) \sim \ln|u^2 - t^2|/2$. Neglecting the higher-order terms, the conductance is

$$\sigma \sim \frac{3}{\pi} \left\{ \alpha + \frac{\sin 3\alpha}{3} + \frac{\alpha^2 \ln \alpha^2}{\pi} \right\}. \tag{30}$$

As shown in Fig. 2, this estimate for σ is reasonably accurate for values of $\alpha < 1$. In the limit when $\alpha \ll 1$, the estimate for σ reduces to linear equation

$$\sigma \sim \frac{6\alpha}{\pi}. \tag{31}$$

As discussed later, this represents the half-space approximation, and is shown in Fig. 2.

B. Approximate solution for σ when $\alpha > 1$

For larger values of α , the integral equation is not amenable to an iterative solution of the type described above. On the other hand, when α becomes large, the perturbation of the heat flow from the uniform flux is not very severe and it is possible to find fairly accurate approximate solutions.

To begin, it is known from the theory of variational calculus that a lower bound for σ can be obtained by suitable mathematical manipulation of the functional given in Eq. (27). To obtain this bound it is necessary to find a vector, say s , that has its divergence equal to zero, and also has no component crossing $r = 1$ in the region $\beta > \theta > \alpha$. This vector can be obtained as the gradient of a function F and the function is harmonic so that $\nabla^2 F = 0$. Such a function can be expressed as a Legendre–Fourier series

$$F = \sum_{n=0}^{\infty} \left\{ \frac{4n+3}{2n+1} \right\} I_{2n+1} P_{2n+1}(\cos \theta) r^{2n+1}. \tag{32}$$

The coefficients I_{2n+1} are chosen so that F satisfies the boundary conditions

$$\frac{\partial F}{\partial r} = \begin{cases} \cos \theta & \alpha > \theta > 0 \\ 0 & \beta > \theta > \alpha \\ \cos \theta & \pi > \theta > \beta \end{cases}. \tag{33}$$

To satisfy this boundary condition, the coefficients I_{2n+1} are expressed by the integrals

$$I_{2n+1} = \int_0^\alpha P_{2n+1}(\cos \theta) \cos \theta \sin \theta d\theta. \tag{34}$$

According to standard treatment,¹⁵ the lower bound for σ is found by suitable mathematical manipulation upon the functional given in Eq. (27). After doing these manipulations, and using the divergence theorem, the bound for σ is given by the following integral which is evaluated on the spherical surface $r = 1$,

$$\sigma = \int_0^\alpha (6T_e - 3F) \cos \theta \sin \theta d\theta, \tag{35}$$

$$= 6I_1 - 3 \sum_{n=0}^{\infty} \left\{ \frac{4n+3}{2n+1} \right\} I_{2n+1}^2.$$

When $\alpha \rightarrow \pi/2$, the summation can be represented by its first term and the estimate for σ reduces to the simple expression

$$\sigma \sim 1 - \cos^6 \alpha. \tag{36}$$

This bound can be improved by multiplying F by a constant say D and then adjusting this constant so as to maximize σ . However, when $\alpha \approx \pi/2$, this refinement does not make much improvement to the estimate for σ . The behavior of this bound is shown in Fig. 2 and, for large values of α , it is in very good agreement with the numerical results.

V. DISCUSSION AND CONCLUSIONS

In a real material, each particle is surrounded on average by N nearest neighbors and $\bar{\alpha}$ is the average cap angle of the contacts. According to their outward normal, these contacts can be partitioned into six different directions $\pm(\hat{i}, \hat{j}, \hat{k})$. In the analysis presented here, the cap angle α is expressed by $\alpha \equiv \bar{\alpha}N/6$. When the contacts are very small in comparison with the size of the particles, the conductance is given by Eq. (31), and $\sigma = \bar{\alpha}N/\pi$. The effective conductivity is then written as

$$k_e = \frac{kfN\bar{\alpha}}{\pi}. \quad (37)$$

This is the same result for the effective conductivity that has previously been deduced by Batchelor and O'Brien.⁴ As the cap angle α increases, the conductance becomes a nonlinear function of α and σ is given approximately by either Eq. (30) or (36).

The present analysis can be related to a unit-cell treatment where the particles are arranged in a simple cubic array. When $\alpha \ll 1$, the spherical particles are barely touching each other and the volume fraction, $f = \pi/6$, then corresponds to simple cubic packing of spheres. Furthermore, according to Eq. (31), the limiting behavior of the conductance is given by $\sigma \sim 6\alpha/\pi$ so that the effective conductivity is $k_e = kf\sigma \sim k_e\alpha$. Now, consider the vertical flow of heat through a simple cubic array. Taking symmetry into account, the four lateral faces are adiabatic while the top and bottom cube faces are isothermal. Thus, when $\alpha \ll 1$, each isothermal contact has a radius approximately equal to α , and, neglecting the curvature of the sphere, the total constriction resistance is $R_c = 1/2k\alpha$. The unit-cell cube has dimensions $2 \times 2 \times 2$, and if its conductivity is k_e then its resistance is $R_e = 1/2k_e$. Upon equating these two resistances, it follows that $k_e = k\alpha$ and this is in agreement with the treatment given here.

As sintering progresses the size of the necks between neighboring particles increases. In the unit-cell model the particle shape has cubic symmetry; the initially spherical particle acquires six facets corresponding to the cube faces. There is no analytical method for deducing the thermal field in such a truncated shape, and it is necessary to resort to a numerical solution. Selecting a spherical test particle has the advantage that it allows a semianalytic solution for the thermal field.

The effective conductivity in Eq. (26) has the simple form $k_e = kf\sigma$, and up to this point, only the behavior of σ

has been considered. The conductance σ depends on the neck growth, whereas the volume fraction f depends on the degree of densification. Ashby¹⁶ points out that there are six distinguishable sintering mechanisms, all causing neck growth. In contrast, only some of mechanisms lead to densification. Although obtaining a general relationship between α and f is beyond the scope of this article, a few remarks are possible. First, during the early stages of sintering there is only neck growth while the f remains constant. Second, at later stages of sintering, corresponding in the analysis to $\alpha \rightarrow \pi/2$, the conductance $\sigma \sim 1$. The effective conductivity is then approximately given as $k_e = kf$ and the model reduces to the law of mixtures. In almost fully dense sintered solids, the porosity exists as isolated spheres and the effective thermal conductivity is better described using Maxwell's¹⁷ estimate instead of the law of mixtures.

ACKNOWLEDGMENTS

Funding for one of the authors (J.R.D.) was provided by NSERC, and, for another author (F.W.Z.), by the Air Force Office of Scientific Research under Contract No. F49620-02-1-0128, monitored by Dr. B. L. Lee.

¹M. Kaviany, *Principles in Heat Transfer in Porous Media* (Springer, New York, 1966).

²S. Torquato, *Random Heterogeneous Materials* (Springer, Berlin, 2002).

³C. K. Chan and C. L. Tien, *ASME J. Heat Transfer* **95**, 302 (1973).

⁴G. K. Batchelor and R. W. O'Brien, *Proc. R. Soc. London, Ser. A* **355**, 313 (1977).

⁵Y. Ogniewicz and M. M. Yovanovich, *Aerodynamic Heating and Thermal Protection Systems*, Progress in Astronautics and Aeronautics, Vol. 59, edited by L. S. Fletcher (American Institute of Aeronautics and Astronautics, 1977).

⁶A. Jagota and C. Y. Hui, *J. Appl. Mech.* **57**, 789 (1990).

⁷J. B. Keller, *J. Appl. Phys.* **34**, 991 (1963).

⁸I. H. Tavman, *Int. Commun. Heat Mass Transfer* **23**, 169 (1996).

⁹C. Argento and D. Bouvard, *ASME J. Heat Transfer* **39**, 1343 (1996).

¹⁰W. W. M. Siu and S. H.-K. Lee, *ASME J. Heat Transfer* **43**, 3917 (2000).

¹¹H. S. Carslaw and J. C. Jaeger, *Conduction of Heat in Solids* (Oxford University Press, Oxford, UK, 1959).

¹²W. D. Collins, *Arch. Ration. Mech. Anal.* **11**, 122 (1962).

¹³I. N. Sneddon, *Mixed Boundary Value Problems in Potential Theory* (North-Holland, Amsterdam, 1966), p. 41.

¹⁴A. P. Prudnikov, Y. A. Brychkov, and O. I. Marichev, *Integrals and Series* (Gordon and Breach, New York, 1966), Vol. 1.

¹⁵A. M. Arthurs, *Complementary Variation Principles*, 2nd ed. (Oxford University Press, Oxford, UK, 1980).

¹⁶M. F. Ashby, *Acta Metall.* **22**, 275 (1974).

¹⁷J. C. Maxwell, *A Treatise on Electricity and Magnetism*, 3rd ed. (Oxford University Press, Oxford, UK, 1904), Vol. 1.